Chemistry
A European
Journal

Chemistry Europe
European Chemical Societies Publishing

Accepted Article

Title: N-aryl amides as chemical exchange saturation transfer magnetic resonance imaging contrast agents

Authors: Xuekang Cai, Jia Zhang, Jiaqi Lu, Long Yi, Zheng Han, Shuixing Zhang, Xing Yang, and Guanshu Liu

To be cited as: *Chem. Eur. J.* 10.1002/chem.202002415

Link to VoR: https://doi.org/10.1002/chem.202002415

WILEY-VCH

10.1002/chem.202002415

WILEY-VCH

COMMUNICATION

N-aryl amides as chemical exchange saturation transfer magnetic resonance imaging contrast agents

Xuekang Cai† [a,b], Jia Zhang† [c,d], Jiaqi Lu[e], Long Yi[b], Zheng Han[c,d], Shuixing Zhang*[f], Xing Yang*[a,g], Guanshu Liu*[c,d]

[a] *Department of Nuclear Medicine, Peking University First Hospital, Beijing, China. E-mail: yangxing2017@bjmu.edu.cn*
[b] *State Key Laboratory of Organic-Inorganic Composites and Beijing Key Lab of Bioprocess, Beijing University of Chemical Technology, 15 Beisanhuan East Road, Chaoyang District, Beijing, China.*
[c] *Russell H. Morgan Department of Radiology, The Johns Hopkins University School of Medicine, Baltimore, Maryland, United States. Email: guanshu@mri.jhu.edu*
[d] *F.M. Kirby Research Center for Functional Brain Imaging, Kennedy Krieger Institute, Baltimore, Maryland, United State.*
[e] *Department of Chemical and Biomolecular Engineering, Johns Hopkins University, Baltimore, Maryland, United States.*
[f] *Department of Radiology, The First Affiliated Hospital of Jinan University, Guangzhou, Guandong, China. Email: shui7515@126.com*
[b] *Institute of Medical Technology, Peking University, Beijing, China*
† These authors contributed equally to this work.
Supporting information for this article is given via a link at the end of the document

Abstract: Chemical exchange saturation transfer (CEST) MRI has recently emerged as a versatile molecular imaging approach in which diamagnetic compounds can be utilized to generate MRI signal. To expand the scope of CEST MRI applications, herein, we systematically investigated the CEST properties of N-aryl amides with different N-aromatic substitution, revealing their chemical shifts (4.6-5.8 ppm) and exchange rates (up to thousands s^{-1}) are favorable to be used as CEST agents as compared to alkyl amide. As the first proof-of-concept study, we used CEST MRI to detect the enzymatic metabolism of the drug acebutolol directly by its intrinsic CEST signal without any chemical labeling. Our study implies that N-aryl amides may enable the label-free CEST MRI detection of the metabolism of many N-aryl amide-containing drugs and a variety of enzymes that act on N-aryl amide, greatly expanding the scope of CEST MR molecular imaging.

Magnetic resonance imaging (MRI) is one of the most commonly used medical imaging modalities. The capacity of MRI for precision diagnosis depends on highly sensitive MRI contrast agents that are designated specifically to the detection of particular molecular targets. Among the currently available MRI contrast mechanisms suitable for molecular imaging, chemical exchange saturation transfer (CEST) is relatively new and versatile, holding great promise for future MR molecular imaging. Instead of paramagnetic metals, CEST MRI utilizes water exchangeable protons to generate specific, sensitive MRI contrast.[1],[2] In particular, the CEST contrast is produced by applying radiofrequency (RF) pulses continuously at the chemical shift of exchangeable protons to completely null the MR signal of these protons (namely saturation). Subsequentially, via proton exchange, these saturated protons will relocate to the surrounding water and transfer the saturation to water, resulting in a detectable level of (water) MRI signal attenuation, which is named CEST contrast.[3] Increasing evidence shows that, with the capability of directly using a broad spectrum of diamagnetic compounds as contrast agents, CEST MRI paves a new avenue to accomplish MR molecular imaging[4]. To date, CEST MRI has been applied to detect anti-cancer drugs,[5] metabolites,[6] amino acids,[7] sugars,[8] and many other important bioorganic agents[9] directly without chemical labeling (namely label-free). Recently, the label-free CEST MRI has also been used to detect enzymatic activity[10]. As the active sites of many biologically relevant enzymes are directly on the exchangeable functional group, one can utilize the difference in the CEST signals between the substrate and product to directly detect the activity of the enzyme of interest. Such an approach, unlike the widely used fluorometric and colorimetric methods, completely eliminates the requirement for chemical labeling and hence favors *in vivo* detection by using the natural substrates of the enzyme as the imaging probe. In this context, a variety of enzymes, including cytosine deaminase (CDase)[10], carboxypeptidase G2[11], proteases[12], protein kinase A[13], deoxycytidine kinase[14], alkaline phosphatases[15], γ-glutamyl transferase (GGT)[16], sulfatase[17], and esterase[18], have been studied. All these studies showed CEST MRI was capable of detecting enzymes in small qualities simply because enzymes can convert the substrates to products continuously without the loss of the enzyme activity, providing a practical way to leverage the sensitivity of CEST MRI.

To expand the scope of CEST MRI applications, it is essential to screen, characterize, select and optimize new types of exchangeable protons and functional groups with desirable CEST properties. In such an investigation, two CEST characteristics are needed to be optimized, i.e., chemical shift (also called CEST offset) and exchange rate, both of which are sensitive to the chemical and physical environment (i.e., pH) around the exchangeable protons. Ideally, the chemical shift ($\Delta\omega$) of the exchangeable proton should be well-separated from the bulk water resonance frequency (set to 0 ppm in MRI convention), and the exchange rate (k_{ex}) should be fast as long as in the slow to intermediate range, i.e., $k_{ex} <= \Delta\omega$. For instance, it has been shown previously that natural phenol[19] and heterocyclic amine[20] can be used for generating CEST MRI contrast with highly shifted chemical shifts. In the present study, we systematically studied the CEST properties of aryl amide, another important type of exchangeable protons, and expanded our knowledge further in the development of CEST-based MR molecular imaging.

Amide proton is one of the most abundant type of exchangeable protons in biomolecules in the human body. With a frequency offset of ~3.5-3.7 ppm apart from water resonance, endogenous alkyl amide has been used for amide proton transfer (APT) imaging, which has entered clinical testing for diagnosing tumors and stroke[21]. The success of APT imaging is attributed to the high concentration of endogenous amide protons in mobile proteins and peptides, despite the exchange rate of alkyl-amide protons typically is slow (~ 30-40 s^{-1})[22], which indeed is not favorable for CEST detectability. Interestingly, recent studies showed a few iodinated X-ray agents, such as Iopamidol and iopromide, can be used as CEST MRI agents, attributable to their inherently carried aryl amide protons [23],[24]. Compared to alkyl amide, these aryl amide protons have larger frequency offsets (i.e., $\Delta\omega$ ~ 5.2-5.6 ppm) and a much faster exchange rate (k_{ex} is ~2560 s^{-1})[23],[24]. Inspired by these studies, we hypothesized that many other N-aryl-amide-containing compounds can be developed as CEST contrast agents with more favorable CEST properties than alkyl amide-containing agents. To this end, we first systematically investigated the CEST properties of a variety of N-aryl amides, characterized the effect of N-aromatic substitution (**Scheme 1**); and then, as the first proof-of-concept study, we used the inherent N-aryl amide CEST signal of

10.1002/chem.202002415

acebutolol, a drug for treating hypertension and arrhythmias, to assess the enzymatic metabolism of acebutolol.

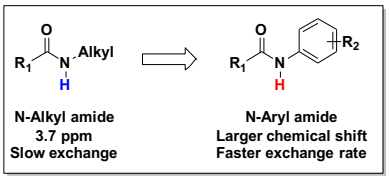

Scheme 1. The rational design of the present study.

We first examined the CEST signal of succinanilic acid, which represents the basic structure of N-aryl amide (**Figure 1A**, with reference to a structure with R_1 = propionic acid and R_2=H in **Scheme 1**). The Z-spectrum and MTR_{asym} plot of succinanilic acid (10 mM in PBS, pH =7.5) were shown in **Figure 1B**, revealing a detectable CEST signal peaked at 4.9 ppm. As shown in **Figure 1C,** N-aryl amide has a strong pH dependence, with the maximum CEST signal =0.9, 2.1, 5.6, and 7.8%, at pH = 6.5, 7.0 and 7.5, and 8.0 respectively. The increase of the CEST signal with pH (**Figure 1D**) is attributed to the faster exchange rates at higher pHs (**Figure 1D insert,** supplementary method), where higher concentrations of OH catalyze the proton exchange.

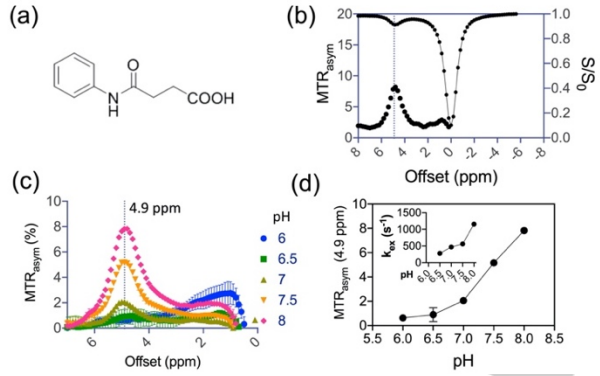

Figure 1. CEST characteristics of succinanilic acid. (a) Chemical structure; (b) CEST signal as depicted by Z-spectrum and MTR_{asym} plot; (c) MTR_{asym} plots at different pH; (d) pH dependence of the peak CEST MRI signal (quantified by MTR_{asym} at 4.9 ppm) and exchange rates (insert). The CEST experiments were performed on a Bruker 9.4 T vertical bore MR scanner with a 25-mm birdcage transmitter/receiver volume RF coil. Unless otherwise noted, all CEST measurements were acquired using a 3-second long, continuous wave (CW) RF pulse with saturation field strength B_1= 3.6 μT (details provided in **supplementary information S2)**.

To elucidate the effect of chemical modifications, we synthesized eighteen different N-aryl amides with different substitutions and studied their CEST properties (supplementary information **S3** and **S4)**. The measured CEST offsets, maximum CEST contrast, and exchange rate are listed in **Table 1** and **Table 2**. Of note, all compounds contain a carboxyl group so as to ensure adequate water solubility >10 mM.

Table 1 summarizes the compounds with *para*- and *meta*-substituted anilides. The largest $\Delta\omega$ was obtained in compounds **5** and **6,** with *para*-electron withdrawing substitutions**,** i.e., 5.2 ppm. The *para*- substitutions only have a small effect on k_{ex}. An electron withdrawing substitution accelerates the exchange rate k_{ex} (**5**-**6**)**,** while an electron-donating substitution slows k_{ex} (**2**). Compared to succinanilic acid (**1**), *meta*-substituted compounds (**7**-**9**) showed similar $\Delta\omega$ (*i.e.,* 5.0 ppm) and slightly faster k_{ex} (*i.e.,* 648 -846 s^{-1}).

In Table 2, *ortho*- Me/MeO- substituted anilides (**10** and **11**) showed slightly reduced $\Delta\omega$ (down to 4.6 ppm) and k_{ex} (down to 320 s^{-1}), likely attributed to electron-donating and steric effect. A relatively large $\Delta\omega$ of 5.6 ppm was seen for compound **15**, indicating the formation of intramolecular hydrogen-bonding between the N-H and ester. To determine the effects of pKa (acidity) of amide protons on the CEST properties, we also calculated the pKa value of each compound (supplementary information **Figure S4.4**) using Advanced Chemistry Development (ACD/Labs) Software V11.02 (1994-2020 ACD/Labs). The results show significantly negative correlation between pKa and k_{ex} (and maximal MTR_{asym} values), indicating that lower pKa (or higher acidity) of aryl amide protons would result in faster exchange and thereby higher CEST signal, whereas no correlation with $\Delta\omega$ (supplementary information **Figure S4.5**). **Table 2** also includes three compounds (**16**-**18**) whose benzene ring is replaced by heterocyclic rings. The heterocyclic substitutions were effective to increase the chemical shifts (up to 5.8 ppm for compound **18**). Compound **18** also exhibited a much faster exchange rate, likely due to dramatically reduced pKa of the N-H.

Overall, chemical modification only has a limited effect on the chemical shift of amide protons, i.e., $\Delta\omega$ varies from 4.6 to 5.8 ppm for all the structures studied. In contrast, the exchange rate and hence the maximum CEST contrast varied greatly. Among all the compounds studied, we found that compound **14** has the highest CEST signal (i.e., 9.7 % in MTR_{asym}, 10 mM at pH 7.4 and 37 °C), which is 1.7-fold higher than that of the model compound succinanilic acid (compound **1**) and more than 3-fold higher than that of compound **2**.

Table 1. CEST properties of *para*- and *meta*-substituted N-aryl amides

Compound	Signal [ppm]	Contrast [%]	k_{ex} [s^{-1}]
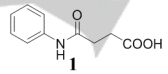 **1**	4.9	5.6	544
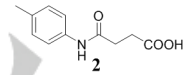 **2**	4.8	2.7	104
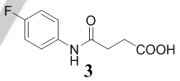 **3**	4.8	5.8	590
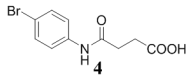 **4**	5	6.2	820
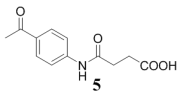 **5**	5.2	6.5	883
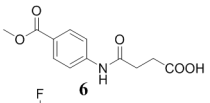 **6**	5.2	7.5	923
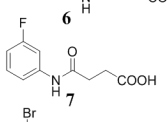 **7**	5.0	7.3	846
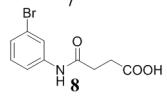 **8**	5.0	7.5	684
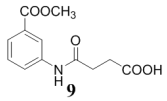 **9**	5.0	7.5	677

The inherent CEST signal of N-aryl amide allows label-free MRI detection of the pharmacokinetics and pharmacodynamics of many N-aryl-amide-containing drugs. To demonstrate it, we chose acebutolol, a β-adrenergic receptor-blocker that is

Table 2. CEST properties of N-aryl amides with ortho- and other heterocyclic substitutions

Compound	Signal [ppm]	Contrast [%]	k_{ex}[s^{-1}]
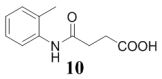 **10**	4.6	5.5	320
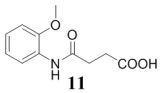 **11**	4.6	7.1	733
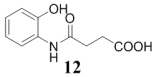 **12**	4.6	8.6	1124
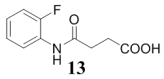 **13**	4.8	8.3	1003
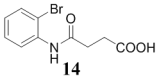 **14**	4.8	9.7	905
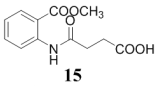 **15**	5.6	7.1	636
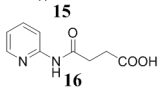 **16**	5.2	7.7	747
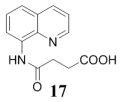 **17**	5.4	3.7	511
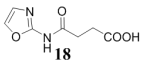 **18**	5.8	3.5	4838

commonly used to treat hypertension and arrhythmia[25]. Acebutolol is a N-aryl amide with two substituents on aromatic ring. While the structure of acebutolol is not a direct derivative of the library compounds listed in Tables 1 and 2, it also contains substituents that tend to enhance the CEST effect as observed in compounds 5 and 11. Indeed, the CEST signal of acebutolol is similar to succinic acid derivatives, with a $\Delta\omega$ of 5.0 ppm, k_{ex} of 959 s^{-1}, and MTR_{asym}=6.3±0.7% for 10 mM acebutolol in PBS, at pH 7.4 and 37 °C. In the liver and intestines, acebutolol is first metabolized to acetolol by carboxylesterases, and subsequently to diacetolol by N-acetyltransferases (**Figure 2a**).[26] The first step of metabolism results in the disappearance of CEST signal at 5 ppm due to the conversion of N-aryl amide to amine, while the second step leads to the re-appearance of the CEST signal (**Figure 2b**). The CEST signals of the substrate acebutolol and final product diacetolol are nearly identical, whereas that of the intermediate product acetolol (synthesized by acid-assisted hydrolysis of acebutolol, supplementary information **S5**) is markedly different, providing a practical way to detect the conversion of acebutolol to acetolol and monitor acetolol-related toxicity caused by N-acetyltransferase deficiency, e.g., lupus erythematosus (DILE).[27]

To demonstrate the capacity of CEST MRI to monitor the enzymatic conversion of acebutolol to acetolol, we first incubated 20 mM acebutolol with carboxylesterase (from porcine liver, Sigma, E3019) at different concentrations for one hour and measured the CEST MRI signal of the reaction systems afterward. As shown in **Figure 2c**, the decrease of the CEST signal at 5 ppm was proportional to the enzyme concentration. At the highest enzyme concentration (*i.e.,* 10 mg/mL), the intensity of CEST signal decreased from 10.4±0.7% to 5.4±1.0%, accounting for a 48% relative signal change. The minimal concentration of enzyme allowing for a reliable CEST detection was determined to be *c.a.* 1 mg/mL (~ 6 μM, MW=168 kD). We then measured the CEST signal change of acebutolol at different concentrations after the incubation with 10 mg/mL esterase for 5 min (**supplementary information S6**), and fitted the data with the Michaelis-Menten kinetic model. The estimated K_M is 93 mM (**Figure 2d**), which is on the same order as the values in the literature, e.g., 29.5 and 238 mM for human liver microsomes and carboxylesterase 1, respectively[26a], demonstrating the ability of CEST MRI to detect enzyme and drug metabolism.

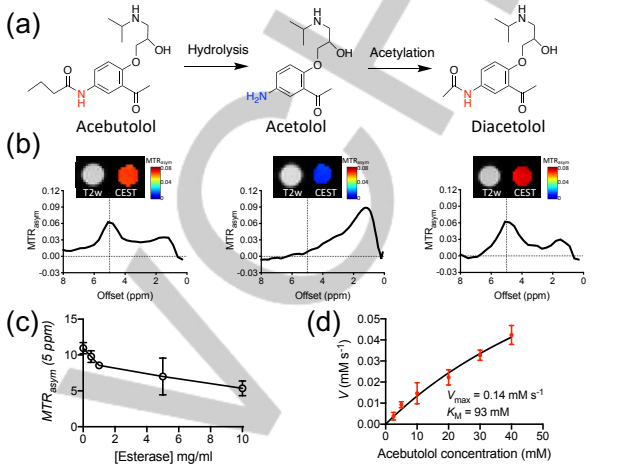

Figure 2. CEST MRI detection of the esterase-catalyzed hydrolysis of acebutolol. (a) *In vivo* metabolic pathway of acebutolol; (b) MTR_{asym} plots of acebutolol, acetolol, and diacetolol in PBS (pH 7.4); (c) CEST signal (quantified by MTR_{asym} at 5 ppm) of 20 mM acebutolol incubated with esterase at different concentrations for 1 h; (d) Fitting CEST MRI data with the Michaelis-Menten kinetic model, in which the initial reaction velocity was calculated using the CEST signal change at each concentration of acebutolol after the first 5 min's incubation. For (b)-(d), all data are averaged on the measurement of three samples, the error bars in (c) and (d) shows the standard deviations. Conditions for CEST MRI acquisition: B_1=3.6 μT/4 s, pH=7.4, 37 °C.

In summary, we systematically investigated the CEST properties of a library of N-aryl amides with different chemical modifications. Compared to alkyl amide, N-aryl amides have further separated chemical shift from water in the range of 4.6-5.8 ppm and much faster exchange rates (up to thousands s^{-1}). The CEST properties of N-aryl amide can be fine-tuned using different chemical modifications. We further demonstrated the application of the CEST signal of N-aryl amide in the label-free MRI detection of the esterase-catalyzed metabolism of a N-aryl amide-containing drug acebutolol. Our study demonstrated that many N-aryl amides can be directly used as CEST agents with favorable CEST properties, which may greatly expand the scope of the biomedical applications of CEST MR molecular imaging.

Acknowledgements

X.Yang is supported by NSFC (21877004) and Clinical Medicine Plus X-Young Scholars Project of Peking University (PKU2020LCXQ029).

Keywords: MRI contrast agent • N-aryl amide • CEST MRI • enzyme detection• acebutolol metabolism

[1] K. M. Ward, A. H. Aletras and R. S. Balaban, *J Magn Reson* **2000**, *143*, 79-87.
[2] J. Y. Zhou and P. C. M. van Zijl, *Progress in Nuclear Magnetic Resonance Spectroscopy* **2006**, *48*, 109-136.
[3] P. C. M. Van Zijl, C. K. Jones, J. Ren, C. R. Malloy and A. D. Sherry, *Proc. Natl. Acad. Sci. USA* **2007**, *104*, 4359-4364.
[4] a) Z. Han and G. Liu, *Wiley Interdiscip Rev Nanomed Nanobiotechnol* **2019**, *11*, e1551; b) G. Liu, S. Ray Banerjee, X. Yang, N. Yadav, A. Lisok, A.

Jablonska, J. Xu, Y. Li, M. G. Pomper and P. van Zijl, *Nat Biomed Eng* **2017**, *1*, 977-982.
[5] a) Y. Li, H. Chen, J. Xu, N. N. Yadav, K. W. Chan, L. Luo, M. T. McMahon, B. Vogelstein, P. C. van Zijl, S. Zhou and G. Liu, *Oncotarget* **2016**, *7*, 6369-6378; b) H. Liu, A. Jablonska, Y. Li, S. Cao, D. Liu, H. Chen, P. C. Van Zijl, J. W. Bulte, M. Janowski, P. Walczak and G. Liu, *Theranostics* **2016**, *6*, 1588-1600; c) L. L. Lock, Y. Li, X. Mao, H. Chen, V. Staedtke, R. Bai, W. Ma, R. Lin, Y. Li, G. Liu and H. Cui, *ACS Nano* **2017**, *11*, 797-805.
[6] K. Cai, M. Haris, A. Singh, F. Kogan, J. H. Greenberg, H. Hariharan, J. A. Detre and R. Reddy, *Nat Med* **2012**, *18*, 302-306.
[7] G. Liu, M. Moake, Y. E. Har-el, C. M. Long, K. W. Chan, A. Cardona, M. Jamil, P. Walczak, A. A. Gilad, G. Sgouros, P. C. van Zijl, J. W. Bulte and M. T. McMahon, *Magn Reson Med* **2012**, *67*, 1106-1113.
[8] T. Jin, H. Mehrens, P. Wang and S. G. Kim, *Neuroimage* **2016**, *143*, 82-90.
[9] D. Ryoo, X. Xu, Y. Li, J. A. Tang, J. Zhang, P. C. M. van Zijl and G. Liu, *Anal Chem* **2017**, *89*, 7758-7764.
[10] G. Liu, Y. Liang, A. Bar-Shir, K. W. Chan, C. S. Galpoththawela, S. M. Bernard, T. Tse, N. N. Yadav, P. Walczak, M. T. McMahon, J. W. Bulte, P. C. van Zijl and A. A. Gilad, *J Am Chem Soc* **2011**, *133*, 16326-16329.
[11] Y. Jamin, T. R. Eykyn, E. Poon, C. J. Springer and S. P. Robinson, *Mol Imaging Biol* **2014**, *16*, 152-157.
[12] M. Haris, A. Singh, I. Mohammed, R. Ittyerah, K. Nath, R. P. Nanga, C. Debrosse, F. Kogan, K. Cai, H. Poptani, D. Reddy, H. Hariharan and R. Reddy, *Sci Rep* **2014**, *4*, 6081.
[13] R. D. Airan, A. Bar-Shir, G. Liu, G. Pelled, M. T. McMahon, P. C. van Zijl, J. W. Bulte and A. A. Gilad, *Magn Reson Med* **2012**, *68*, 1919-1923.
[14] Z. Han, Y. Li, J. Zhang, J. Liu, C. Chen, P. C. van Zijl and G. Liu, *Cancer Res* **2019**, *79*, 2775-2783.
[15] I. Daryaei, M. M. Ghaffari, K. M. Jones and M. D. Pagel, *ACS Sens* **2016**, *1*, 857-861.
[16] S. Sinharay, E. A. Randtke, K. M. Jones, C. M. Howison, S. K. Chambers, H. Kobayashi and M. D. Pagel, *Magn Reson Med* **2017**, *77*, 2005-2014.
[17] S. Sinharay, G. Fernandez-Cuervo, J. P. Acfalle and M. D. Pagel, *Chemistry* **2016**, *22*, 6491-6495.
[18] R. Thomas, *Chembiochem* **2016**, *17*, 2293.
[19] a) X. Yang, X. Song, Y. Li, G. Liu, S. R. Banerjee, M. G. Pomper and M. T. McMahon, *Angew Chem Int Ed Engl* **2013**, *52*, 8116-8119; b) J. Zhang, Y. Yuan, Z. Han, Y. Li, P. C. M. van Zijl, X. Yang, J. W. M. Bulte and G. Liu, *Biosens Bioelectron* **2019**, *141*, 111442.
[20] X. Yang, X. Song, S. Ray Banerjee, Y. Li, Y. Byun, G. Liu, Z. M. Bhujwalla, M. G. Pomper and M. T. McMahon, *Contrast Media Mol Imaging* **2016**, *11*, 304-312.
[21] H. Zhu, C. K. Jones, P. C. van Zijl, P. B. Barker and J. Zhou, *Magn Reson Med* **2010**, *64*, 638-644.
[22] a) J. Zhou, D. A. Wilson, P. Z. Sun, J. A. Klaus and P. C. Van Zijl, *Magn Reson Med* **2004**, *51*, 945-952; b) H. Y. Heo, Z. Han, S. Jiang, M. Schar, P. C. M. van Zijl and J. Zhou, *Neuroimage* **2019**, *189*, 202-213.
[23] S. Aime, L. Calabi, L. Biondi, M. De Miranda, S. Ghelli, L. Paleari, C. Rebaudengo and E. Terreno, *Magn Reson Med* **2005**, *53*, 830-834.
[24] S. Sinharay, E. A. Randtke, C. M. Howison, N. A. Ignatenko and M. D. Pagel, *Mol Imaging Biol* **2018**, *20*, 240-248.
[25] W. H. Frishman, *American Heart Journal* **1987**, *113*, 1190-1198.
[26] a) K. Muta, T. Fukami and M. Nakajima, *Biochem Pharmacol* **2015**, *98*, 659-670; b) U. Rakibe, R. Tiwari, A. Mahajan, V. Rane and P. Wakte, *J Pharm Anal* **2018**, *8*, 357-365.
[27] S. Fenniche, A. Dhaoui, F. B. Ammar, R. Benmously, H. Marrak and I. Mokhtar, *Skin Pharmacol Physiol* **2005**, *18*, 230-233.

10.1002/chem.202002415

WILEY-VCH

COMMUNICATION

Entry for the Table of Contents

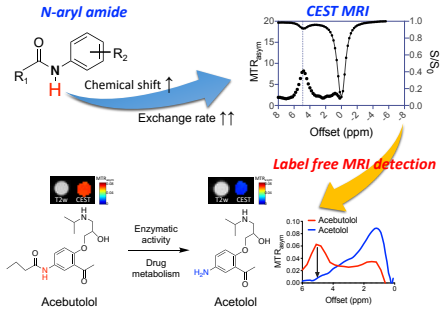

The chemical exchange saturation transfer (CEST) MRI properties of N-aryl amides were systematically investigated. With relatively large chemical shifts and fast exchange rate, this type of diamagnetic, biocompatible compounds can be directly used as CEST agents for label-free MRI detection of enzymatic activity and drug metabolism.